論文2003-40TC-6-2

OFDM시스템을 위한 적응 문턱값 설정방식의 심볼동기화 알고리듬

A Symbol Synchronization Algorithm With an Adaptive Threshold Establishment Method For OFDM Systems

宋 東 鎬 *, 周 昌 福 *

(Dong-Ho Song and Chang-Bok Joo)

요 약

제안된 알고리듬은 채널 잡음전력에 따라 적응적으로 문턱값 레벨을 결정하는 적응 문턱값 설정방식을 사용하여 채널특성에 관계없이 항상 최적의 문턱값을 설정한다. 또한, 이것은 그 추정성능이 다중경로채널에서의 전력지연 프로파일 변동에 대해 덜 민감하도록 만드는 특별하게 설계된 훈련심볼을 사용한다. 그 결과, 제안된 기법의 추정성능은 채널특성 변동에 대해 영향을 적게 받는다.

Abstract

The proposed algorithm can always set up the optimal threshold value regardless of channel characteristics using an adaptive threshold establishment method that determines the threshold level according to channel noise power, and then it uses the specially designed training symbols that can make the algorithm's estimation performance be less sensitive to power delay profile variation in a multipath channel. In result, the estimation performance of the proposed technique is less affected by channel characteristic variation.

Keywords : OFDM, symbol synchronization, adaptive threshold establishment method, moving subtraction method, edge detection method.

I. INTRODUCTION

Orthogonal frequency-division multiplexing(OFDM)[1-4] has been adopted or expected for a number of applications, from asymmetric digital subscriber line (ADSL)[5] to the next-generation mobile communication and home networking systems.

In OFDM systems, the synchronization includes carrier frequency synchronization and timing recovery. Timing recovery is further divided into symbol synchronization and sampling clock synchronization. The purpose of symbol synchronization is to find the correct position of the fast Fourier transform (FFT) window.

Usually, symbol synchronization can be achieved with the aid of the dedicated training symbols or the periodic property of guard interval. In this paper, we present the symbol synchronization algorithm using

* 正會員, 慶南大學校 電子工學科

(Dept. of Electronic Engineering Kyungnam University)

※ 본 논문은 경남대학교 학술연구지원에 의해 수행되어졌습니다.

接受日字:2003年2月17日, 수정완료일:2003年5月24日

the training symbols.

Symbol synchronization techniques are divided into the correlation-based methods[6-9] and subtraction-based methods[10-12] typically. However, the correlation-based methods have the disadvantage that is to be sensitive to channel characteristic in the estimation performance. That is, in the cross-correlation methods that correlate between the training symbols stored at the receiver and those received via channel, peak position and value vary as channel delay profile. Moreover, the performance of the auto-correlation methods that correlate between the training symbols received via channel and the version delayed by the period of the training symbols is influenced by not only channel characteristic but a threshold value. Actually, because the optimal threshold value of such methods is different every channel and SNR, it is difficult to set up the value that is suitable for any channel environments. However, the proposed algorithm that is based on the subtraction method can always set up an optimal threshold value regardless of channel characteristics using an adaptive threshold establishment method that determines the threshold level according to channel noise power, and then it uses the specially designed training symbols that can make the algorithm's estimation performance be less sensitive to power delay profile variation in a multipath channel, thereby the proposed algorithm's performance is less affected although channel characteristic varies in the condition that the established threshold value is kept. In conclusion, the proposed algorithm can provide more stable and better symbol synchronization performance on the practical channel environments that we do not know in advance.

This paper is organized as follows. In Section II, we describe the OFDM signal and channel model that is necessary for analysis of the proposed algorithm. In Section III, we analyze the proposed algorithm. Section IV presents the simulation results and analysis, and Section V concludes the paper.

II. OFDM SIGNAL AND CHANNEL MODELS

Consider an OFDM system which consists of N subcarriers.

Let $X_{i,k}$ represents the subcarrier symbols where i represents the OFDM symbol number and k represents the subcarrier number as $k=0,1,\ldots,N-1$. N is also identical with the IFFT (FFT) point number (N_{FFT}) as the data sample number in time domain.

At the transmitter, the N symbols are modulated onto the N subcarriers via an IFFT. The cyclic prefix is also added in the guard interval to avoid ISI caused by multipath fading. As a result, the output signal of the transmitter can be given as[13]

$$x(t)=\sum_{i=-\infty}^{\infty}\sum_{k=0}^{N-1}X_{i,k}\Psi_{i,k}(t) \tag{1}$$

where $\Psi_{i,k}(t)$ is the subcarrier pulse. That is,

$$\Psi_{i,k}(t)=\begin{cases} e^{j2\pi f_k(t-T_{GI}-iT_{sym})}, & iT_{sym}\le t\le (i+1)T_{sym}, \\ 0, & otherwise \end{cases} \tag{2}$$

where $T_{sym}=T_{FFT}+T_{GI}$ is the duration of an OFDM symbol including the guard interval, $f_k=k/T_{FFT}$ is the kth subcarrier frequency, T_{FFT} is the FFT period, and T_{GI} is the guard interval period.

We assume that the signal is transmitted on a multipath fading channel characterized by

$$h(\tau,t)=\sum_{l=0}^{L-1}h_l(t)\delta(\tau-\tau_l) \tag{3}$$

where $h_l(t)$ is the lth path complex gain, τ_l is the lth path time delay ($\tau_0=0$), and L is the total number of paths.

At the receiver, if we assume the ideal high power

amplifier characteristic and perfect OFDM synchronization, the received down-converted signal can be written as

$$y(t)=\sum_{l=0}^{L-1}h_l(t)x(t-\tau_l)+w(t) \quad (4)$$

where $w(t)$ represents the Additive White Gaussian Noise whose mean is zero and variance is $\sigma_w{}^2$. When (4) is sampled at $t=iT_{sym}+nT_s=iT_{sym}+nT_{FFT}/N$, during the ith OFDM symbol, the nth sampled signal can be represented by

$$y(i,n)=\sum_{l=0}^{L-1}h_l(i,n)x(i,n-d_l)+w(i,n) \quad (5)$$

where $n=-N_G,\cdots,-1,0,1,\cdots,N-1$ are sample indices, T_s is the sampling time interval, $d_l=\tau_l/T_s$ is the lth path sample delay, and $N_G=T_G/T_s$ is the cyclic prefix sample number added in the guard interval.

In indoor and outdoor environments, the maximum Doppler frequency is usually very small compared with the subcarrier frequency. Therefore, we can assume that during the ith OFDM symbol, the channel impulse response scarcely change. That is,

$$h_l(iT_{sym}+nT_s)\approx h_l(i) \quad (6)$$

If we consider only one OFDM symbol to simplify (5), it will be able to be written as

$$y(n)\approx\sum_{l=0}^{L-1}h_lx(n-d_l)+w(n) \quad (7)$$

Ⅲ. PROPOSED SYMBOL SYNCHRONIZATION ALGORITHM

In the proposed algorithm, the ideal timing position is just the first sample of GI2, which is the guard interval of length $2N_G$ for long training symbols made up of two consecutive symbols (L1, L2) of each length N in <Fig. 1.> We call it the base symbol timing position θ_0 and consider the base symbol timing error as $e_\theta=\hat{\theta}-\theta_0$ where $\hat{\theta}$ is the estimated base symbol timing position in a packet. Actually, $\hat{\theta}$ is applied to the FFT window controller, and on the basis of it, the controller finds out the position of the FFT block in each OFDM symbol in a packet. Thus, we can simply call $\hat{\theta}$ a estimated symbol timing.

1. Training symbols constitution

In this paper, we present the constitution of training symbols as <Fig. 1.> The presented training symbols consist of short training symbols, training symbols for symbol synchronization, and long training symbols. The training symbols for symbol synchronization constitute one OFDM symbol including its guard interval. That is, the OFDM symbol consists of the guard interval (GI) of length N_G and two identical training symbols (T1, T2) of each length N_{TRS} (=N/2). The structures of the short and long training symbols are the same as those of IEEE 802.11a PLCP preamble[14]. Moreover, the training symbols for symbol synchronization are generated by the elements of sequence with indices that are a multiple of 2 have non-zero amplitude; +1 or -1, and then the short and long training symbols are generated by the IEEE 802.11a short and long sequence[14].

In ideal case, the proposed algorithm determines the next sample position of the null duration of <Fig. 1> as symbol timing position with a threshold value.

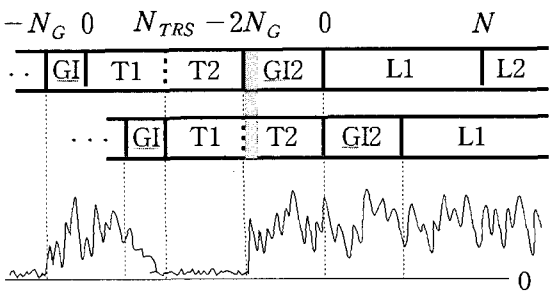

그림 1. 훈련심볼 구성
Fig. 1. The training symbols constitution.

However, in the practical case of existing noise, because the threshold value is applied according to the difference-noise power, the difference power of the corresponding samples that are within the shadowy region must be high to guarantee the superior performance regardless of channel characteristic variation. Therefore, we can generate the training symbols that can make to obtain the desired results as we arrange the sequence elements (+1, 0, -1) of generating the training symbols in frequency domain so that training symbols itself have the high difference-signal power within the shadowy region. However, because such constitution of the training symbols are related to peak-to-average power ratio, we must consider this in designing systems. In this paper, the training symbols with PAPR=4.3656dB is used. The size of the shadowy region can be only one sample provided the power of the first difference signal within the region is sufficiently large compared with the difference power of noise at low SNR (e.g., 5dB or 0dB). However, the proposed algorithm uses the moving average process that make to smother the power value of the difference signal and then to make the performance of the algorithm be more stable, we should make the sample number within the region be roughly the moving average window length. In conclusion, the presented training symbols' constitution can make the proposed algorithm's estimation performance be less sensitive to the relative power difference variation of path-components in a multipath channel.

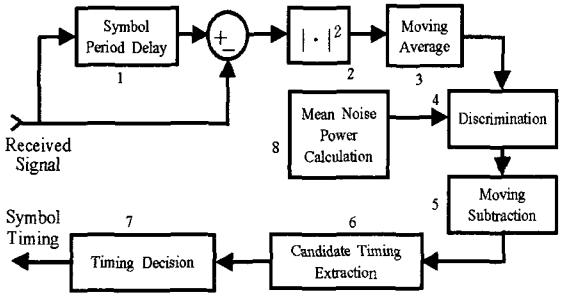

그림 2. 제안된 심볼타이밍 추정기
Fig. 2. Proposed Symbol Timing Estimator.

2. Proposed Algorithm with the Training Symbols

The signals at the each stage of the proposed symbol timing estimator of <Fig. 2> are presented below.

1) Difference Signal

Consider $|\tau_M/T_s - N_G| = N_{I-f}$ where τ_M is the maximum delay spread of channel and N_{I-f} is the number of the ISI-free samples in the guard interval. The received signal in (7) is subtracted from itself that is delayed by the training symbol period, N_{TRS}. In result, the difference signal, $y_{diff}(n)$ can be written as

$$\begin{aligned} y_{diff}(n) &= y(n-N_{TRS}) - y(n) \\ &\approx \sum_{l=0}^{L-1}[h_l x(n-N_{TRS}-d_l) + w(n-N_{TRS}) \\ &\quad - h_l x(n-d_l) - w(n)] \end{aligned} \tag{8}$$

However, since $x(n-N_{TRS}) = x(n)$ in $N_{TRS} - N_{I-f} \le n < N$, $x(n-N_{TRS}-d_l) = x(n-d_l)$.

2) Power Signal

The power signal, $|y_{diff}(n)|^2$ becomes

$$|y_{diff}(n)|^2 \approx \begin{cases} |w_{diff}(n)|^2 = |w(n)|^2 + |w(n-N_{TRS})|^2 \\ \quad -2*real[w(n)^* w(n-N_{TRS})], \\ \quad N_{TRS} - N_{I-f} \le n < N, \\ |\sum_{l=0}^{L-1}[h_l\{x(n-N_{TRS}-d_l) - x(n-d_l)\}] \\ \quad + w_{diff}(n)|^2, \\ \quad otherwise. \end{cases} \tag{9}$$

Note the first equation. Within $N_{TRS} - N_{I-f} \le n < N$, the power signal is approximated as the difference-noise power signal; $|y_{diff}(n)|^2 \approx |w_{diff}(n)|^2$. This represents that the proposed algorithm's threshold level can be determined only by the noise power.

3) Moving Average(MA)

The moving average of $|y_{diff}(n)|^2$ is calculated as

$$y_{avg}(n)=\frac{1}{L_{MA}}\sum_{m=0}^{L_{MA}-1}|y_{diff}(n-m)|^2 \quad (10)$$

where L_{MA} is the moving average window length. Its optimal value will be determined by simulation. The moving average process is used to decrease noise effects that generate unwanted zero duration in discriminator output.

4) Discrimination

Discrimination process of $y_{avg}(n)$ is as follows.

$$y_{disc}(n)=\begin{cases}1, & y_{avg}(n)\geq P_{th},\\ 0, & y_{avg}(n)<P_{th}\end{cases} \quad (11)$$

where P_{th} is the threshold value. We need to determine the optimal P_{th}. This is calculated on the basis of (9). It is important that P_{th} should be larger than the maximum value of $|y_{diff}(n)|^2\approx|w_{diff}(n)|^2$ in $N_{TRS}-N_{I-f}\leq n<N$. If this condition is not satisfied, unwanted '1' duration is generated in wanted '0' duration. It has moving subtracter extract incorrect timing information. However, because it seldom come within the range where it is determined by timing decision part as correct timing, it is not finally detected as symbol timing signal.

Because $w(n)$ and $w_{diff}(n)$ are Wide-sense stationary random processes, the follow equation is reasonable.

$$E[\frac{1}{L_{MA}}\sum_{m=0}^{L_{MA}-1}|w_{diff}(n-m)|^2]=E[\ |w_{diff}(n)|^2\ ]$$
$$=\sigma^2_{w_{diff}}$$
$$\approx 2\sigma^2_w\approx 2\alpha^2\sigma^2_{w'} \qquad N_{TRS}-N_{I-f}\leq n<N, \quad (12)$$

where α is the fixed VGA (Variable Gain Amplifier) gain after AGC (Automatic Gain Controller) stabilizes within previous training symbols duration and $\sigma^2_{w'}$ is the additive noise variance that is estimated in the packet detector when an effectual signal is not received.

By simulation, the optimal P_{th} range is determined. The simulation result 2 of Section IV will show the timing error distribution characteristics with various P_{th} values. In result, we can approximately adopt the optimal P_{th} range as

$$3.0\sigma^2_{w_{diff}}\leq P_{th}\leq 3.5\sigma^2_{w_{diff}} \quad (13)$$

or

$$3.0\times 2\sigma^2_w\leq P_{th}\leq 3.5\times 2\sigma^2_w \quad (14)$$

where $\sigma^2_{w_{diff}}$ and σ^2_w are the variance of $w_{diff}(n)$ and $w(n)$ respectively. Furthermore, the optimal threshold value can be adopted as follows.

$$P_{opth}=3.2\sigma^2_{w_{diff}} \text{ or } P_{opth}=3.2\times 2\sigma^2_w \quad (15)$$

where the optimal coefficient of 3.2 is constant regardless of channel characteristic and SNR. That is, the threshold value only depends on noise power.

This standard for setting up the threshold level provides a stable threshold value in any unfixed channel environment contrary to the conventional techniques such as the methods of detecting a minimum value or determining the fixed threshold level via simulations on various channels. That is, this approach does not detect the minimum value from the subtraction result for the estimation of a symbol timing but ultimately takes an instant crossing a threshold with a few samples following after the minimum value as a symbol timing, and hence if we make training symbols so that the strength of those samples is high, the errors of the estimates for the symbol timing will be reduced. Futhermore, the proposed algorithm rather reinforces the power strength of such samples with the interference by multipath signals, and this characteristic is proven from the second formula of Eq. (9). Therefore, providing that we constitute the training symbols as <Fig. 1> and use the proposed

adaptive threshold establishment method, the estimation performance of a symbol timing becomes not only better but also freer from the influence of noise within the null duration in <Fig. 1.> Besides, these characteristics cause it to be shorten the length of the moving average (MA) window to reduce the effects of noise.

5) Moving Subtraction(MS)

We introduce moving subtraction method that is used as the detection technique of timing information. The method performs subtraction operation between an original signal and its delayed signals every sample as

$$y_{MS}(n) = y_{disc}(n) - \sum_{m=1}^{L_{MS}-1} y_{disc}(n-m) \quad (16)$$

where L_{MS} is the length of the moving subtraction window. That is, MS method is similar to the rising edge detection (RED) method. However, as compared with RED method, MS method can reduce the generation probability of negative timing error because the samples of amplitude +1 with the preceding null duration which is smaller than L_{MS} do not affects the estimation of the desired timing instant via MS process as <Fig. 3.> This can make the subcarrier symbols be less influenced by ISI when the our algorithm achieves symbol synchronization. Therefore, we use MS technique to detect timing information. The detection principle of MS method is presented in <Fig. 3>[15].

In determining L_{MS}, we have to consider the loss possibility of the desired timing. That is, when unexpected noise is added, as L_{MS} grows larger, the loss possibility of the expected timing becomes higher. Therefore, we determine L_{MS} as

$$L_{MS} = 3. \quad (17)$$

This equation represents that MS method has its minimum function. For reference, we can make MS method operate like RED method. In this case, the moving subtraction window length is 2; $L_{MS} = 2$.

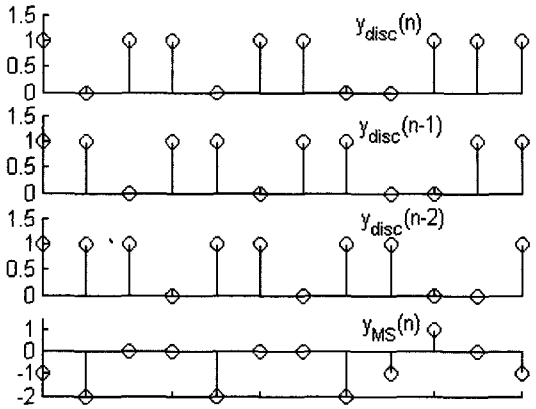

그림 3. MS방식의 검출원리

Fig. 3. The detection principle of MS method ($L_{MS} = 3$).

6) Candidate Timing Extraction

The candidate timing extraction is achieved by passing only the positive part of $y_{MS}(n)$. That is, $y_{MS}(n) = 1$ only go out like that, and others become '0'. The passed $y_{MS}(n)$ is the unit impulse function at the sample time of nT_s. Therefore, it is just candidate timing signal, and the then n is candidate timing position. In hardware, the timing extractor can be simply composed of a comparator.

7) Timing Decision

We assume that signal (or packet) detection error or another preceding reference timing's error can be in the range of $n \leq |E_{\lim}|$ where $E_{\lim}$ is the error limit in the unit of sample. The timing decision part recognizes the extracted candidate timing as the counted sample ordinal number in a packet and detects the proper timing by the follow conditions:

$$D_{TLB} = N_{pre} + N_G + N + 1 - E_{\lim} + E_{pkd} \quad (18)$$

and

$$D_{TUB} = N_{pre} + N_G + N + 1 + E_{\lim} + E_{pkd} \quad (19)$$

where D_{TLB} is the Timing Decision Lower Bound, D_{TUB} is the Timing Decision Upper Bound in the unit of sample, N_{pre} is the sample number from the

true packet start to the end of the training symbols that go before those for symbol synchronization, and E_{pkd} is packet detction error within the $-E_{\lim} \le E_{pkd} \le E_{\lim}$. That is, the candidate timing that precedes D_{TLB} is removed and the first one that is entering between D_{TLB} and D_{TUB} is detected in real-time processing. If no candidate timing has existed between D_{TLB} and D_{TUB}, the algorithm produces either forced timing on basis of the packet detection information or a false alarm. However, this case hardly happens provided the algorithm's parameters are optimum. Therefore, we consider θ to be in the range of $D_{TLB} \le \theta \le D_{TUB}$. Because the ideal timing estimate position θ_0 is $N_{pre}+N_G+N+1$, the distribution range of timing estimate error ($e_\theta = \theta - \theta_0$) can be written as $-E_{\lim}+E_{pkd} \le e_\theta \le E_{\lim}+E_{pkd}$.

Ⅳ. SIMULATION RESULTS AND ANALYSIS

In this section, we show the simulation results that are necessary to set up the optimal parameters of the proposed algorithm and demonstrate the algorithm's performance by computer simulation on two multipath channels: channel I and channel II that have the different power delay profile.

<Fig. 4.> shows the power delay profiles of two channels that have the normalized maximum delay spreads of $\tau_{\max}/T_s = 7$ and $\tau_{\max}/T_s = 17$ respectively.

The OFDM system parameters used in the simulation are the same as those in IEEE standard 802.11a PHY specification[14]. That is, $T_{sym} = 4\mu s$, $T_{FFT} = 3.2\mu s$, $T_{GI} = 0.8\mu s$, and $T_s = 50ns$. Therefore, $N_{sym} = 80$, $N = 64$, and $N_G = 16$. Besides, we assume that packet detection error can be in the range of $n \le |E_{\lim}|$ and that $E_{\lim} = 8$.

In simulation, $\sigma^2_{w_{diff}}$ is vicariously calculated by

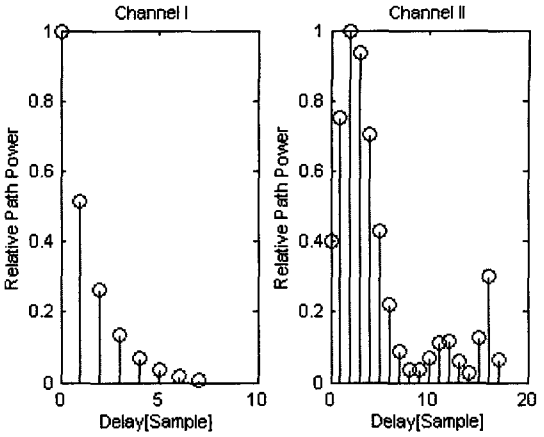

그림 4. (a) 채널 I 과 (b) 채널 II의 전력지연 프로파일
Fig. 4. The power delay profile of (a) channel I and (b) channel II.

$\sigma^2_{w'}$ as in (15). This will be precise if the sample number of difference-noise power signal $|w_{diff}(n)|^2$ for averaging is sufficient. We can thereby use the follow equation to calculate $\sigma^2_{w_{diff}}$ for given SNR[dB] value; $\sigma^2_{w_{diff}} \approx 2\alpha^2\sigma^2_{w'} = 2\alpha^2\sigma^2_{r'} \times 10^{-(SNR[dB]/10)}$ where $\sigma^2_{r'}$ is the variance of the received signal excluding additive noise before entering the AGC process, and we assume that it is normalized to '1'. Moreover, we suppose that $\alpha = 1$ for convenience. The calculated $\sigma^2_{w_{diff}}$ is applied to threshold value setting up.

All results were obtained by averaging over 200 Monte Carlo trials.

Simulation Result 1: We first observe Fig. 5 to find out the optimal L_{MA}. This figure shows the mean square error (MSE) performance curves of the proposed algorithm with various P_{thc} values versus L_{MA} with various P_{thc} values at SNR=5dB and SNR=7dB in AWGN channel (No CFO).

L_{MA} change at SNR=5dB and 7dB on the AWGN channel where P_{thc} is the coefficient of P_{th}; $P_{th} = P_{thc}\,\sigma^2_{w_{diff}}$. From Fig. 5, we can find out that MSE value grows larger as L_{MA} grows larger or becomes smaller centering around $L_{MA} = 4$. This is because the moving average less reduces the effects

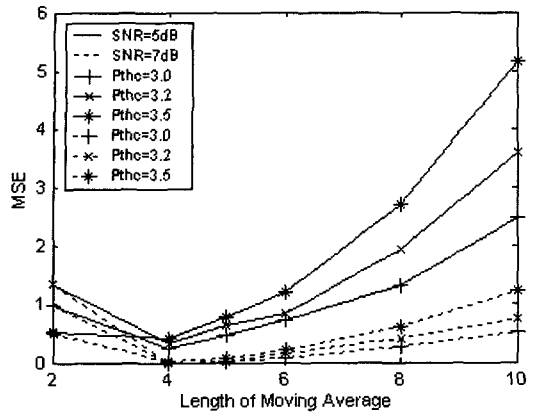

그림 5. AWGN 채널에 대해 SNR=5dB 와 7dB에서의 P_{thc}값들에 따른 L_{MA} 대 심볼타이밍의 MSE 특성

Fig. 5. Mean square value of symbol timing error vs. L_{MA} with various P_{thc} values at SNR=5dB and SNR=7dB in AWGN channel(No CFO).

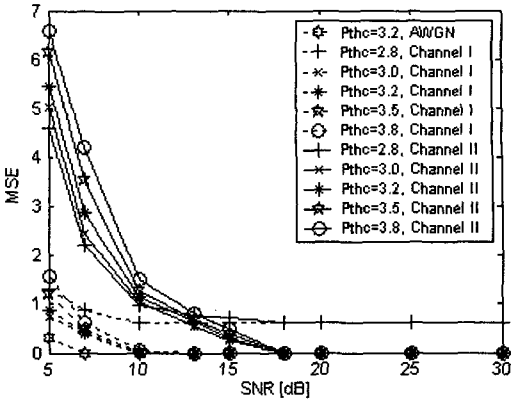

그림 6. AWGN 채널, 채널 I 과 II 에서의 P_{thc}값들에 따른 SNR 대 심볼타이밍의 MSE 특성

Fig. 6. Mean square value of symbol timing error vs. SNR[dB] with various P_{thc} values in AWGN channel, channel I, and channel II ($L_{MA}=4$, No CFO).

of noise as L_{MA} becomes smaller and it more smooths the amplitude of the signal; $|y_{diff}(n)|^2$ as L_{MA} grows larger. Therefore, we must find out the optimal value of L_{MA}. If possible, it has to be small because the difference-signal power corresponding to the shadowy region of Fig. 1 must be high even after moving average process to guarantee the better estimation performance of the proposed algorithm. Futhermore, at the optimal value, the MSE values have to be nearly constant with various P_{thc} values because in such cases, the distribution characteristic of timing estimate errors is most stable even in threshold-value fluctuation by calculation error of mean difference-noise power ($\sigma^2_{w_{diff}}$) corresponding to a variation of the presented P_{thc}. Hence, we consider the optimal L_{MA} as $L_{MA\_OPT}=4$ where the MSE values with various P_{thc} values are most similar.

Simulation Result 2: We shall then find out the optimal range and value of P_{thc} at $L_{MA\_OPT}=4$ that is the optimal length of moving average window. Fig. 6 shows the mean square error(MSE) versus SNR[dB] with various P_{thc} values and various channels in the proposed symbol timing estimation algorithm. From this figure, we can see that the MSE curves with $P_{thc}=2.8$ show error floor in both channels. This happens because the negative timing errors exist. That is, this result represents that $P_{thc}=2.8$ is not large enough to overcome the effects of noise. Thus, we exclude $P_{thc}=2.8$ from the optimal range of P_{thc}. However, P_{thc} must not be too large because the larger positive timing errors are generated as P_{thc} grows larger. Thereby, the smaller P_{thc} should be selected if possible. In conclusion, we consider the optimal range of P_{thc} as $3.0 \le P_{thc} \le 3.5$ and the rough median of the optimal range as the optimal value of P_{thc}, $P_{opthc}=3.2$. By these results, it is proved that (13), (14), (15) are reasonable. However, the practically calculated $\sigma^2_{w_{diff}}$ can be different with the theoretical value, but even so, provided the threshold value($P_{th}=3.2\sigma^2_{w_{diff}}$) is within the optimal threshold value range, our algorithm can maintain the superior timing estimation performance. That is, centering around (15), (13) can be written as $3.2\sigma^2_{w_{diff}}-0.2\sigma^2_{w_{diff}} \le P_{th} \le 3.2\sigma^2_{w_{diff}}$,

$+0.3\,\sigma^2_{w_{diff}}$and from this, we can analogize that the calculation tolerance of $\sigma^2_{w_{diff}}$ is about $\pm 10\%$ of the theoretical value.

Additionally, we can see that the proposed algorithm with $P_{opthc}=3.2$ and $L_{MA\_OPT}=4$ can achieve the ideal symbol timing estimation performance over SNR=7dB in AWGN channel, over SNR=10dB in channel I, and SNR=18dB in channel II.

Simulation Result 3: In this simulation result, we compare the estimation performance of our method having the optimal parameters ($L_{MA}=4$ and $P_{thc}=3.2$) with that of the other correlation-based methods. Fig. 7(a) shows the MSE performance curves of our method and the typical auto-correlation based method (Minn's sliding window method[9]) versus SNR[dB] in channel I and channel II. From this figure, we can see that there is all the difference between the MSE performance of our method and that of the Minn's sliding window method. This occurs because in auto-correlation based methods as in[9], the timing-error means are shifted to the right in time axis by some amount depending on the channel delay spread and the timing-error variance curves form error floor owing to the ISI influences of multipath channels. In short, the proposed algorithm has far superior MSE performance than the presented auto-correlation method. Fig. 7(b) then shows the MSE performance curves of our method and the cross-correlation based methods (using the different training symbols; short and long training symbols [14]) versus SNR[dB] in channel I and channel II. In the presented methods taking the cross-correlation process, the search window for the peak detection is the same as $E_{pkd}+N_p-(E_{\lim}+1)\le\theta\le E_{pkd}+N_p+E_{\lim}-1$ where N_p is the sample number corresponding to the distance from packet start position to ideal symbol timing estimation position. In the same as our method, $E_{\lim}=8$. From Fig. 7(b), we can see that in channel I, our method has similar MSE performance to that of the other methods and has the ideal MSE performance of '0' over SNR=10dB. In channel II, both MSE performance curves of the two cross-correlation methods form error floors, but our method has the ideal performance (MSE=0) over SNR=18dB. And then, Fig. 7(b) shows that the MSE performance of the cross-correlation method using the long training symbols[14] is worse than that using the short training symbols. This means that more correlation samples do not always guarantee better performance in multipath channels. Besides, we can find out that our method has better MSE performance than the two cross-correlation methods over the specific SNR (about 10dB in both channels).

Simulation Result 4: We next compare the probability distribution of symbol timing error of our method having the optimal parameters ($L_{MA}=4$ and $P_{thc}=3.2$) with that of the correlation based methods presented in Fig. 7. Fig. 8 shows the probability distribution histograms of symbol timing error with various methods on channel I and channel II at SNR=5dB. From Fig. 8(b) and (f) about Minn's sliding window method[9], we can see that the distribution of timing errors is shifted to right in time axis by some amount owing to the ISI influences of multipath channels as stated above. Furthermore, from Fig. 8(c) and (g), we can find out that in the cross-correlation method using the short training symbols[14], the timing estimate errors are distributed within the peak search range that depends on the signal(packet) detection range and are much differently distributed according to channels at the same SNR. On the other hand, as in Fig. 8(a) and (e), the timing-error distribution of our method is not so much affected by channel characteristic variation. and keeps within the bounds from 0 to +4. When we compare this with the distribution characteristics of Fig. 8(d) and (h), we can see that the proposed algorithm's performance is less dependent upon channel characteristic compared with the cross-correlation method's performance using the long

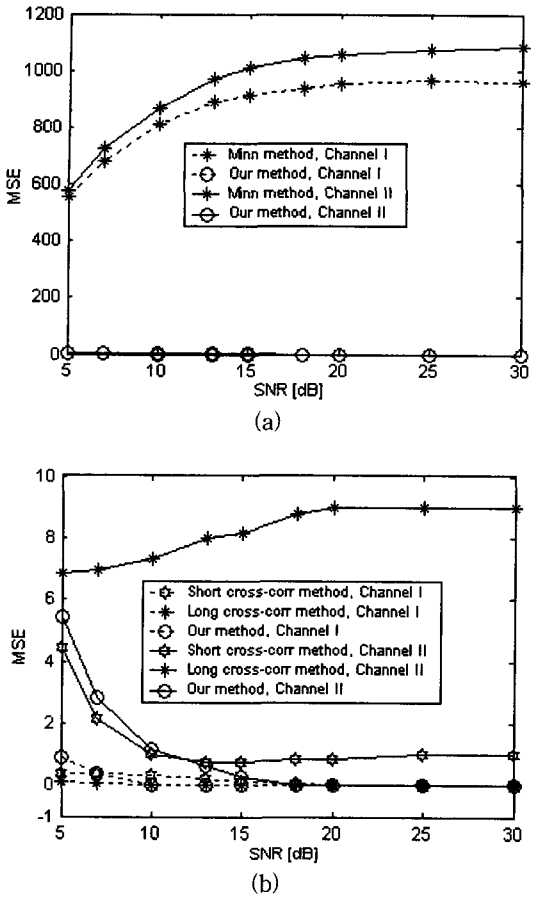

그림 7. 채널 I 과 II 에 대해 제안된 방식과 (a) 자기상관 방식 (b) 상호상관 방식간의 SNR 대 심볼타이밍의 MSE 비교

Fig. 7. Comparison our methods with (a) auto-correlation method and (b) cross-correlation methods; Mean square value of symbol timing error vs. SNR[dB] in channel I and channel II ($L_{MA}=4$, $P_{thc}=3.2$, No CFO).

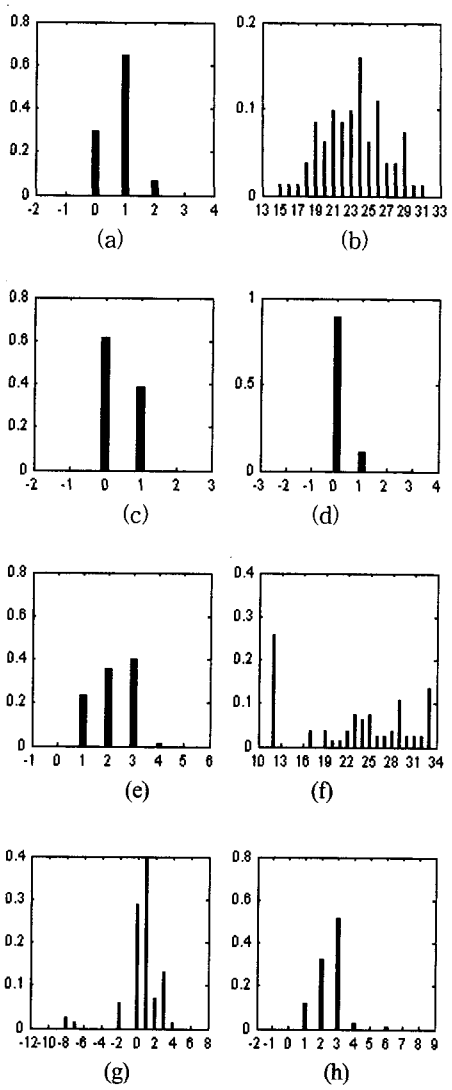

그림 8. 채널 I(좌측)과 채널 II(우측)에 대해 SNR=5dB 에서의 여러 타이밍 추정방식들에 대한 추정에러의 확률분포 비교

Fig. 8. The probability distribution vs. timing error [sample] of various timing estimation methods at SNR=5dB; (a) and (e) in our method, (b) and (f) in Minn's sliding window method[9], (c) and (g) in short training symbols cross-correlation method, and (d) and (h) in long training symbols corss-correlation method on channel I and channel II respectively ($L_{MA}=4$, $P_{thc}=3.2$, No CFO).

training symbols[14]. Besides, from Fig. 8, we can find out that the proposed method's distribution characteristic is rather more stable than that of the rest of the cross-correlation methods although the MSE values of our method are larger than those of the others at low SNRs as in Fig. 7(b). In conclusion, we can consider that our method is less affected by channel characteristic variation compared with the presented correlation based methods.

Simulation Result 5: By this time, all simulation results have been performed in the ideal condition of no carrier frequency offset (CFO). Fig. 9 shows the effects of CFO in the proposed algorithm with the

optimal parameters on channel II at SNR=5dB, 10dB, and 20dB. The optimal parameters are $L_{MA}=4$ and $P_{thc}=3.2$. In this figure, NCFO denotes the carrier frequency offset that is normalized by subcarrier spacing. At SNR=5dB, as NCFO increase in the positive direction or in the negative direction in the vicinity of NCFO=0, the mean timing error (MTE) value grows larger or becomes smaller, but the variance of the timing estimate error does not so much change. That is, when NCFO is between -0.1 and +0.1, the distribution characteristic of the timing estimate error is somewhat different but the estimation performance of the proposed algorithm is scarcely degraded. Likewise, we can find out that the estimation performance of the proposed algorithm is hardly degraded by the effects of CFO when NCFO is between -0.06 and +0.06 at SNR=10dB, between -0.015 and +0.015 at SNR=20dB respectively.

Provided a remaining NCFO after coarse CFO synchronization is done is in these range of NCFO, the proposed algorithm can be very effectively used in wireless systems. Usually, a remaining NCFO after coarse CFO synchronization is approximately below 0.052, 0.027, and 0.008 at SNR=5dB, 10dB, and 20dB respectively. Hence, our algorithm is robust to a residual carrier frequency offset.

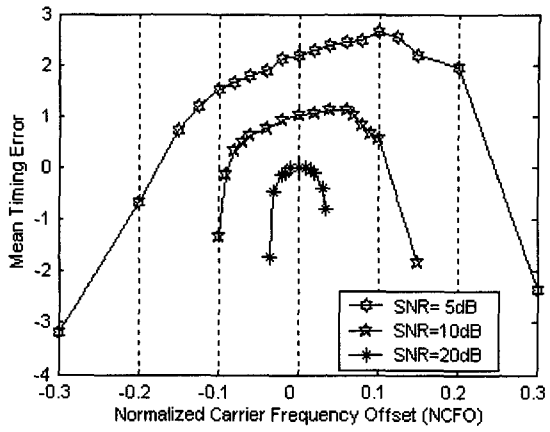

(a)

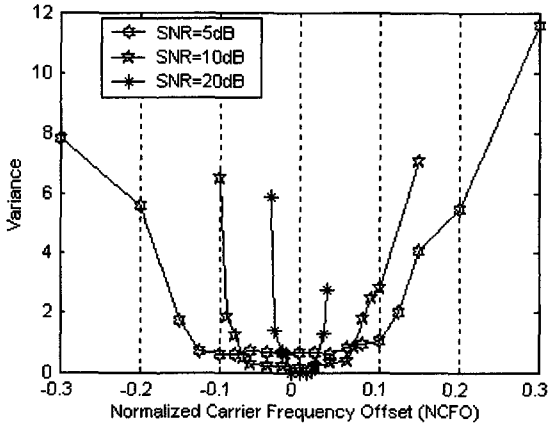

(b)

그림 9. 채널 II에 대한 $P_{thc}=3.2$인 제안된 추정 알고리듬의 NCFO 대 (a)평균 타이밍 에러 특성 (b) 타이밍 에러의 분산 특성

Fig. 9. (a) Mean and (b) Variance of symbol timing error vs. NCFO in the proposed estimation algorithm with $P_{thc}=3.2$ in channel II ($L_{MA}=4$, $SNR=5dB$, $10dB$, and $20dB$).

V. CONCLUSION

In this paper, we have proposed the symbol synchronization algorithm with the adaptive threshold establishment method for OFDM systems. The proposed algorithm is less sensitive to the relative power difference variation of path-components in a multipath channel compared with conventional correlation-based methods. Simulation result 3 and 4 demonstrated this. In particular, Simulation result 4 shown that even at low SNR; 5dB, the variance of symbol timing error is small in both channels. In short, our algorithm can provide more stable and better symbol synchronization performance on the practical time-variant channel environments that we do not know in advance. Besides, the proposed algorithm has a small amount of computation because its operation is based on a subtraction process and its moving average window length is only 4. These characteristics also solve a problem of the necessity of a long moving average window that is one of disadvantages of conventional subtraction methods.

REFERENCES

[1] A. Peled and A. Ruiz, "Frequency domain data transmission using reduced computational complexity algorithms," in Proc. IEEE ICASSP 80, Denver, CO, pp. 964~967, 1980.

[2] L. J. Cimini, "Analysis and simulation of a digital mobile channel using orthogonal frequency division multiplexing," IEEE Trans. Commun., vol. 33, pp. 665~675, July 1985.

[3] M. Alard and R. Lassalle, "Principles of modulation and channel coding for digital broadcasting for mobile receivers," EBU Tech. Review, no. 24, pp. 3~25, Aug. 1987.

[4] J. A. C. Bingham, "Multicarrier modulation for data transmission: an idea whose time has come," IEEE Commun. Mag., vol. 28, pp. 17~25, Mar. 1990.

[5] Asymmetric digital subscriber line (ADSL) metallic interface. ANSI Standard T1. 413~1995.

[6] J. J. van de Beek, M. Sandell, M. Isaksson, and P. O. Borjesson, "Low-complex frame synchronization in OFDM systems," in Proc. IEEE Int. Conf. Universal Personal Commun., pp. 982~986, Nov. 1995.

[7] T. M. Schmidl and D. C. Cox, "Low-overhead, low-complexity [burst] synchronization for OFDM," in Proc. IEEE ICC, pp. 1301~June 1996.

[8] T. M. Schmidl and D. C. Cox, "Robust frequency and timing synchronization for OFDM," IEEE Trans. Commun., vol. 45, no. 12, pp. 1613~Dec. 1997.

[9] H. Minn, M. Zeng, and V. K. Bhargava, "On timing offset estimation for OFDM systems," IEEE Commun. Lett., vol. 4, no. 7, pp. 242~244, July 2000.

[10] P. J. Tourtier, R. Monnier, and P. Lopez, "Multicarrier modem for digital HDTV terrestrial broadcasting," Signal Processing, pp. 379~Dec. 1993.

[11] M. Speth, F. Classen, and H. Meyr, "Frame synchronization of OFDM systems in frequency selective fading channels," in Proc. IEEE VTC, pp. 1807~1811, May 1997.

[12] K. Takahashi and T. Saba, "A novel symbol synchronization algorithm with reduced influence of ISI for OFDM systems," in Proc. IEEE GLOBECOM, vol. 1, pp. 524~528, 2001.

[13] B. Yang, K. B. Letaief, S. Cheng, and Z. Cao, "Timing recovery for OFDM transmission," IEEE J. Select. Areas Commun., vol. 18, no. 11, pp. 2278~2291, Nov. 2000.

[14] IEEE, Wireless LAN Medium Access Control (MAC) and Physical Layer (PHY) specifications: High Speed Physical Layer in the 5 GHz band. IEEE Std 802.11a-1999, Nov. 2000.

[15] D. H. Song, S. H. Cho, W. J. Lee, and C. B. Joo, "A Symbol Synchronization Algorithm for OFDM Systems Using the Moving Subtraction Method," in Proc. IEEE TENCON'02, vol. II, pp. 933~937, Oct. 2002.

저 자 소 개

宋 東 鎬(正會員)

2001년 2월 : 경남대학교 전자공학과 학사. 2001년 3월~현재 : 경남대학교 전자공학과 석사과정. <주관심분야 : 디지털 통신시스템, 통신신호처리>

周 昌 福(正會員)

1981년~현재 : 경남대학교 전기전자공학부 교수. 1975년 : 한국항공대학교 전자공학과 학사. 1977년 : 고려대학교 전자공학과 공학석사. 1987년 : 고려대학교 전자공학과 공학박사. 1987년 : 일본 상지대 전자공학과 연구교수. 1992년 : 미국 일리노이주립대 시카고교 전자컴퓨터공학과 객원교수. <주관심분야 : 이동통신, 통신시스템 및 통신 신호처리>